Progress In Electromagnetics Research, PIER 78, 83–101, 2008

MULTIPLE UWB EMITTERS DOA ESTIMATION EMPLOYING TIME HOPPING SPREAD SPECTRUM

J. P. Lie and B. P. Ng

Nanyang Technological University
School of Electrical and Electronic Engineering
50 Nanyang Ave. Block S2, Singapore 639798

C. M. S. See

DSO National Laboratories
20 Science Park Drive, Singapore 118230

Abstract—In this paper, UWB Direction of Arrival (DoA) estimation using channelization receiver architecture proposed in [1] is extended to cover the case of multiple UWB emitters employing Time Hopping Spread Spectrum (TH-SS) multiple access technique. The DoA estimation is based on the spectral lines extracted from the channelizer. When considering the multiple-emitter case, these spectral lines are dependent on the hopping sequences assigned to the emitters (as derived in [2]). The principle behind the proposed method is to set the channelizer's frequencies at which only the spectral lines from the desired UWB emitter are present while those from the other emitters are absent. This requires a proper design of the hopping sequences that govern the transmission of all emitters. First, an additive white Gaussian noise channel is considered to demonstrate the fundamental principle. Then, the estimation in a realistic multipath channel is addressed. Simulation results show that the direction finding function successfully indicates the DoA of the desired signal when the channelizer's frequencies are set for the detection of that signal.

1. INTRODUCTION

For the last decade, there has been a growing interest in Ultra Wideband (UWB) radio technology. The transmission of nanosecond pulse in the baseband has attracted a lot of attentions from many researchers in the field of radar-related applications. Recently, the

focus of research on UWB radio technology has been diversified to the field of wireless communications [3–5] and localization [6, 7]. It offers the benefits of high data rate communication due to its very wide bandwidth and high resolution localization capability, while keeping low hardware cost.

To realize a UWB localization system, time delay estimation has been proposed while direction of arrival (DoA) technique is not popular (conventional narrowband array processing concept [9, 10] does not apply for UWB). Recently, a UWB DoA estimation technique has been proposed using a digital channelization receiver [1]. The receiver consists of an UWB antenna array and a channelizer. The channelizer splits the sum of the received signals at the array to multiple frequency bands and then down-converts them to much lower frequency such that a low sampling rate ADC can be used for sampling. Thus, Nyquist rate sampling for the complete UWB bandwidth is not required. The use of low sampling rate ADC also helps to reduce the computational complexity of the estimation.

Utilizing the receiver structure, we propose a method to estimate the DoA in multiple access communications. The UWB multiple access technique considered in this paper is Time Hopping Spread Spectrum (TH-SS) multiple access technique as proposed in [4]. The basic principle of the proposed method is to set the channelizer's frequencies such that only the spectral lines from the desired UWB emitter will contribute to the channelizer's frequencies.

First, an additive white Gaussian noise (AWGN) channel is considered. The TH sequences are assigned to the active emitters. These sequences are designed such that the resulting spectral lines of the signal transmitted by one emitter are spectrally separable from the signal transmitted by the others. The design of the TH sequences is presented as a maximization of a derived objective function.

Then, the estimation in a realistic multipath channel is addressed. In view of the multiple replicas of the UWB pulse received due to multipaths, we propose to use a simple multipath suppression technique that detects and locates the leading edge of the first-arrival multipath component. This technique is implemented at the RF front-end of each sensor of the array. Therefore, the direction finding (DF) function computed after the multipath suppression will indicate only the DoA of the first-arrival multipath component.

The rest of this paper is organized as follows. In Section 2, the signal model for multiple UWB emitters' transmission is given. Section 3 reviews the single emitter UWB DoA estimation and the digital channelization receiver structure. The proposed multiple emitters DoA estimation technique is described in Section 4, covering

both the AWGN and multipath case. In Section 5, simulation results are discussed. Finally, the paper is concluded in Section 6.

2. SIGNAL MODEL

In multiple-user transmission employing TH-SS, the transmission signal model of the q-th emitter is given by [2]

$$s_q(t) = \sum_{j=-\infty}^{\infty} w_{tx}\left(t - jT_f - c_j^{(q)}T_c\right) \tag{1}$$

where $w_{tx}(t)$ is the transmitted pulse waveform, j and T_f are the frame index and frame interval, respectively, T_c is the chip interval and $c_j^{(q)}$ symbolizes the hopping sequence of the q-th user. That is, the transmitted signal is a train of pulses positioned at different time instants, which are defined by the hopping sequence. Without loss of generality, the data modulation in the transmission is omitted.

The hopping code is of limited length (denoted as N_f), which is also the number of frames representing one information symbol. Since only one pulse is transmitted within one frame duration, the number of pulses used for representing one symbol is also N_f. Thus the periodicity of the transmission is $N_f T_f$. There are N_f pulses in one period of transmission and each pulse is time-shifted by $c_j^{(q)}T_c$ where $c_j^{(q)}$ is an integer values between 0 and $N_h - 1$. Also, one frame interval is divided equally into N_h chip intervals where $N_h = \frac{T_f}{T_c}$. Figure 1 illustrates the q-th emitter's transmission employing TH-SS.

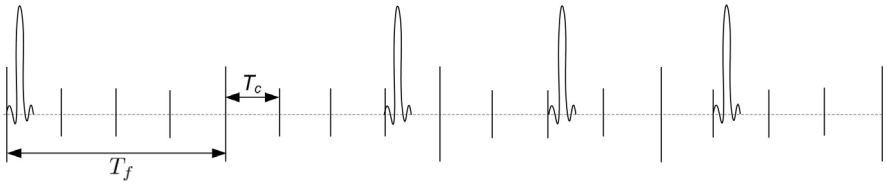

Figure 1. Illustration of the q-th user transmission employing TH-SS. The hopping sequence deduced from the illustration is $\{0, 3, 2, 1\}$ where $N_h = 4$.

Consider an N-element UWB antenna array receiving UWB signal wavefronts $s_q(t)$ where $q = \{1, \cdots, Q\}$, emitted from K active sources.

The total received signal of the n-th antenna is:

$$r_n(t) = \left[\sum_{q=1}^{Q} \alpha_q \sum_{l=1}^{L_q} a_l^{(q)} s_q(t - \tau_{toa}^{(q)} - \tau_l^{(q)} - \tau_{l,n}^{(q)}) \right] + \eta(t) \qquad (2)$$

where α_q and $\tau_{toa}^{(q)}$ are the path loss attenuation and the Time of Arrival (ToA) of the q-th user, $a_l^{(q)}$ and $\tau_l^{(q)}$ are the fading coefficients and delays of the multipath components due to the q-th user's transmission, respectively. $\tau_{l,n}^{(q)}$ is the differential delay due to the l-th multipath component of the q-th signal

$$\tau_{l,n}^{(q)} = \frac{x_n \sin(\theta_l^{(q)}) + y_n \cos(\theta_l^{(q)})}{c} \qquad (3)$$

where (x_n, y_n) is the n-th antenna's two dimensional position and c is the speed of light. $\eta(t)$ denotes a zero-mean AWGN noise with power spectral density (PSD) $N_o/2$. The expression $s_q(t)$ is similar to (1), except that the pulse waveform is now $w_{rx}(t)$.

For the AWGN channel assumption, there is no multipath component received at the array, or $L_q = 1\ \forall q$. For the multipath channel assumption, we consider the following constraints when addressing the problem

- The chip interval is long enough to let the multipath dies out within the chip interval, or $T_p + \tau_{L_q} < T_c\ \forall q$ where T_p is the pulse duration.
- The hopping sequence assigned to one emitter is unique to other emitters. That means, within any chip interval, there will be only one pulse transmitted.

3. BACKGROUND: UWB DOA ESTIMATION FOR SINGLE UWB EMITTER

In this section, the DoA estimation technique for the single emitter case using the channelizer is reviewed in order to provide the necessary background for further discussions.

The sum of the received signals at the array can be expressed simply as

$$y(t) = \sum_n r_o(t - \tau_n) \qquad (4)$$

where the propagation channel is assumed to be AWGN and only one emitter is transmitting and $r_o(t) = s(t - \tau_{toa})$. τ_n is the differential delay measured with respect to the ToA of the signal at 0-th antenna located at the array phase center. Transforming (4) into frequency domain, we arrive at

$$Y(\omega_m) = R_o(\omega_m) \sum_n \exp(-i\omega_m \tau_n) \tag{5}$$

where $R_o(\omega_m)$ is the spectrum of the received signal at the 0-th antenna and i denotes $\sqrt{-1}$. Note that $\{\omega_1, \cdots, \omega_M\}$ covers the frequency band of UWB signal. The channelized expression in (5) can be represented in a matrix form

$$\mathbf{y} = \text{diag}\{\mathbf{r}_o\}\mathbf{A}\mathbf{1}_{N\times 1} \tag{6}$$

where $\mathbf{y} = [\ Y(\omega_1) \quad \cdots \quad Y(\omega_M)\ ]^T$ and $\mathbf{r_0} = [\ R_o(\omega_1) \quad \cdots \quad R_o(\omega_M)\ ]^T$ are the spectral vectors of the array output and the array phase center, respectively; $\mathbf{A} = [\ \mathbf{a}_0 \quad \cdots \quad \mathbf{a}_{N-1}\ ]$, where $\mathbf{a}_n = \left[\ e^{-i\omega_1\tau_n} \quad \cdots \quad e^{-i\omega_M\tau_n}\ \right]^T$ and $\mathbf{1}_{N\times 1}$ is a column vector of all elements equal to 1. Note that $[\cdot]^T$ denotes transpose.

To extract the DoA, a general optimization approach is used. The final derivation leads to a mathematical representation

$$\hat{\theta} = \arg\min_{\theta_s} |\mathbf{P}_C^{\perp}\mathbf{y}| \tag{7}$$

where $\mathbf{P}_C^{\perp} = \mathbf{I} - \mathbf{C}\left(\mathbf{C}\mathbf{C}^H\right)^{-1}\mathbf{C}^H$ and $\mathbf{C} = \text{diag}\{\mathbf{r_o}\}\mathbf{A}$ (the superscript H denotes matrix conjugate transpose and $\mathbf{I}$ denotes identity matrix). θ_s denotes the scanning direction.

The channelization process is implemented using the structure shown in Figure 2 as proposed in [1]. This process can be summarized as follows

(i) Let f_m denote the m-th frequency value of the channelizer and f_o denote the center frequency of Bessel Band Pass Filter (B-BPF). The m-th mixer is then tuned to $f_{xm} = f_m - f_o$, where output of the mixer can be written as

$$y_{xm}(t) = y(t) \times \exp(-i2\pi f_{xm} t) \tag{8}$$

Note that f_m is set to the frequency that gives maximum power, which can be realized using a tunable oscillator

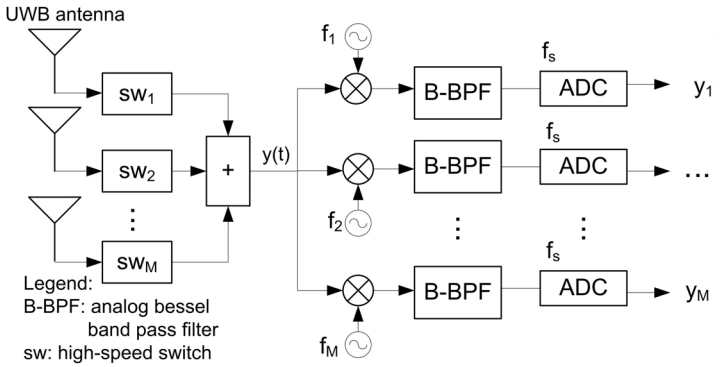

Figure 2. The proposed channelization receiver architecture.

(ii) Filtering by B-BPF of center frequency f_o, whose impulse response is denoted by $h(t)$

$$y_{fm}(t) = y_{xm}(t) \otimes h(t) \tag{9}$$

where $\otimes$ denotes the convolution operation.

(iii) Sampling with $f_s = 4f_o$

$$y_m[n] = y_{fm}\left(\frac{n}{f_s}\right), \quad -\infty < n < \infty \tag{10}$$

(iv) Taking N_{sh} snapshots at m-th branch and performing Discrete Fourier Transform

$$c_m = \frac{1}{N_{sh}} \sum_{n=0}^{N_{sh}-1} y_m[n] e^{-i\left(\frac{2\pi}{N_{sh}}\right)mn} \tag{11}$$

(v) Taking m-th Fourier coefficients, where $m = N_{sh}/4$

$$Y(\omega_m) = c_{(N_{sh}/4)} \tag{12}$$

The channelizer results in M complex values forming the vector $\mathbf{y}$. In order to form the vector $\mathbf{r}_o$, the received signal at the array phase center is input to the channelizer as seen from Figure 2. High-speed switches are implemented at each array elements. When all switches are closed, the vector $\mathbf{y}$ is formed and when only the switch of the receiving antenna at the array phase center is closed, the vector $\mathbf{r}_o$ is formed. Alternatively, two channelizers can be implemented to form each vector.

4. MULTIPLE UWB EMITTERS DOA ESTIMATION

In the presence of multiple UWB emitters, the received signals at the array have been given in (2) and the expression of the sum of them in (4) is no longer valid. Instead, the sum is now

$$y(t) = \sum_n \sum_q \alpha_q \left\{ r_{1,o}^{(q)}(t - \tau_{1,n}^{(q)}) + \sum_{l=2}^{L_q} r_{l,o}^{(q)}(t - \tau_{l,n}^{(q)}) \right\} \tag{13}$$

where $r_{l,o}^{(q)}(t)$ is the received multipath signal due to the transmission from the q-th user propagating from the l-th path at the array phase center

$$r_{l,o}^{(q)}(t) = a_l^{(q)} s_q(t - \tau_{toa}^{(q)} - \tau_l^{(q)}) \tag{14}$$

Note that if an AWGN channel is considered, the transmitted signal propagates only from one path. Thus, the received signal contains only one DoA. Otherwise if a multipath channel is considered, multiple DoAs are observed at the array. We first discuss the AWGN case, and then the multipath case.

4.1. AWGN Channel

In an AWGN channel, the sum of the received signal at the array expressed in (13) can be simplified as

$$y(t) = \sum_n \sum_q \alpha_q r_o^{(q)}(t - \tau_{1,n}^{(q)}) \tag{15}$$

where the received signal at one sensor is a time-shifted signal at the other's sensor. Transforming (15) into frequency domain, we arrive at

$$Y(\omega_m) = \sum_q R_o^{(q)}(\omega_m) \sum_n \exp(i\omega_m \tau_{1,n}^{(q)}) \tag{16}$$

For the purpose of illustration, we consider the first user as the user-of-interest and the rest as multiple access interference (MAI). Thus, (16) can be re-expressed as

$$Y(\omega_m) = R_o^{(1)}(\omega_m) \sum_n \exp(-i\omega_m \tau_{1,n}^{(1)}) + I_{MAI}(\omega_m) \tag{17}$$

$$I_{MAI}(\omega_m) = \sum_{q=2}^{Q} R_o^{(q)}(\omega_m) \sum_n \exp(-i\omega_m \tau_{1,n}^{(q)}) \tag{18}$$

In order to cancel the MAI, the principle idea is to design the TH sequences such that $R_o^{(q)}(\omega_m) = 0$ for $q = \{2, \cdots, M\}$. Since the channelization process extracts the spectral lines only at $\{\omega_1, \cdots, \omega_M\}$, we can search for the TH sequences that is minimized at these frequencies only.

The general expression of the spectrum of a TH signal has been analyzed in [2]. Therefore, is given by

$$R_o^{(q)}(2\pi f) = \left\{ \frac{\alpha_q}{N_f T_f} \right\}^2 |W(2\pi f)|^2 \times \left| \sum_{j=0}^{N_f-1} e^{i2\pi f(jT_f + c_j^{(q)} T_c)} \right|^2 \times \sum_{k=-\infty}^{\infty} \delta_D \left(f - \frac{k}{N_f T_f} \right) \times e^{i2\pi f \tau_{toa}^{(q)}} \tag{19}$$

where $W(2\pi f)$ is the Fourier transform of the received pulse waveform $w_{rx}(t)$ and $\delta_D(t)$ is the Dirac delta function. The expression is composed of multiple line spectra separated by the reciprocal of $N_f T_f$. Overall, the spectrum is determined by both the received pulse waveform and the TH code.

We define $C_q(f)$ as the sum of the code-dependent terms in (19) as

$$C_q(f) = \left| \sum_{j=0}^{N_f-1} \exp(-i2\pi f(jT_f + c_j^{(q)} T_c)) \right|^2 \tag{20}$$

We can further simplify (20) by first expanding it using Euler's formula and then re-expressing it using trigonometric equalities. Thus, we arrive at the following expression (see Appendix for a detailed derivation)

$$C_q(f) = N_f + \sum_{j_1=0}^{N_f-1} \sum_{j_2=0}^{N_f-1} \cos[2\pi(\rho_q T_c) f] \tag{21}$$

where we define ρ_q as

$$\rho_q = N_h(j_1 - j_2) + c_{j_1}^{(q)} - c_{j_2}^{(q)} \tag{22}$$

Because the spectrum is a discrete line representation, the continuous frequency index f can be replaced with the discrete frequency index k

using the relationship $f = k/(N_f T_f)$. The formula in (21) is now

$$C_q(k) = N_f + \sum_{j_1=0}^{N_f-1} \sum_{j_2=0}^{N_f-1} \cos\left[2\pi \frac{\rho_q}{N_f N_h} f\right] \tag{23}$$

To find the frequencies $\{\omega_1, \cdots, \omega_M\}$, at where the spectrum of the user-of-interest can be extracted, given the TH codes, we define a search criterion to find the discrete index k. If the user-of-interest is user 1, the search is given by

$$k_1 = \arg\max_k C_1(k) - \sum_{q=2}^{Q} C_q(k) \tag{24}$$

Note that the search range of k is limited to the integer values from 1 to $N_f N_h$. This is because the sum of the code-dependent terms is periodic in $N_f N_h$. Therefore, we need to find only one discrete frequency. For the purpose of illustration, consider two users transmission employing the TH codes $\{5, 5, 2, 2\}$ and $\{0, 6, 4, 2\}$, generated pseudo-randomly, for user 1 and 2, respectively. The other transmission parameters are $T_f = 80$ns and $T_c = 10$ns. If user 1 is the user-of-interest, the search defined in (24) resulted in $k_1 = 16$. Otherwise, the search resulted in $k_2 = 8$. If translated back into the continuous frequency, when the user-of-interest is user 1, the frequencies are $f^{(1)} = \{100\mathbb{Z}^+ + 50\}$MHz where $\mathbb{Z}^+ = \{0, 1, 2, 3, \cdots\}$. By selecting the channelizer's frequencies to be a subset of $f^{(1)}$, we can cancel the MAI's spectrum. Likewise, when the user-of-interest is user 2, the frequencies are $f^{(2)} = \{100\mathbb{Z}^+ + 25\}$MHz.

Figure 3 shows the PSD of user 1, user 2 and the total received signal at the frequencies subset of $f^{(1)}$ and $f^{(2)}$. It can be seen that the spectral lines of user 1 can be extracted from the total received signal PSD at $f^{(1)}$, and vice versa. These observations suggest that the DoA estimation technique described in Section 3 can be used to estimate the DoA of the desired emitter at the presence of transmitted signals from the other emitters by simply setting the channelizer's frequencies to the desired emitter's unique frequency series.

Earlier on, we have formulated an objective function to search for the discrete frequency k in (24). The objective function is at maximum when the sum of the user-of-interest's code-dependent terms is maximized while that of the MAI is nullified. From the simplified expression of the sum of code-dependent terms in (23), we can deduce that it is maximized when all the cosine terms are 1 and the maximum value is N_f^2.

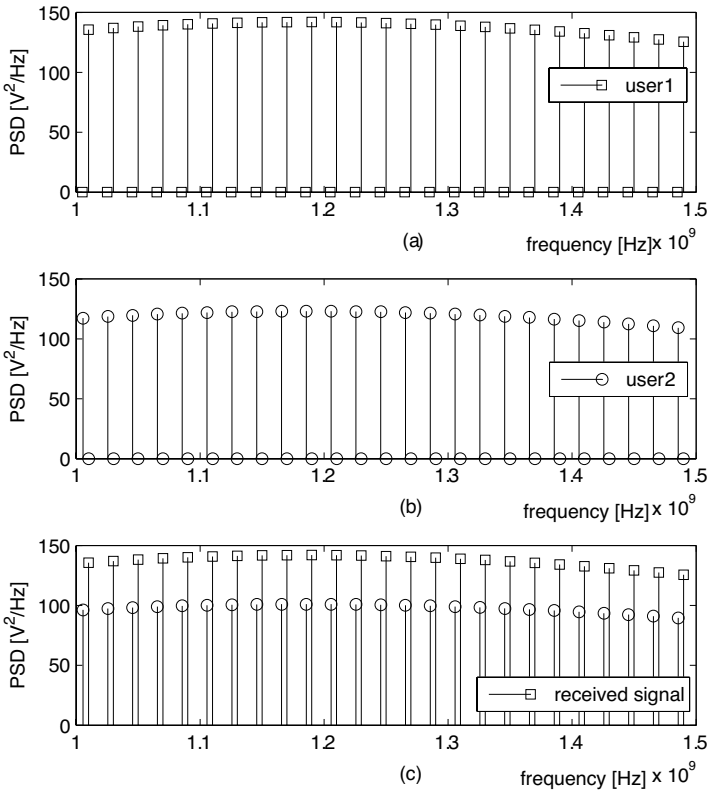

Figure 3. The PSD of the transmitted signal from (a) user 1 only employing $c_j^{(1)} = \{5, 5, 2, 2\}$, (b) user 2 only employing $c_j^{(2)} = \{0, 6, 4, 2\}$ and (c) both users at frequencies subset of $f^{(1)}$ and $f^{(2)}$.

Given the two TH codes $c_j^{(1)}$ and $c_j^{(2)}$, the objective function reaches its maximum value. However, when more emitters are considered, it is difficult to find the set of the TH codes that gives the maximum objective function. Therefore, we define an efficiency factor ϵ that measures the ratio of the calculated value of the objective function to the maximum value. For example, if the user-of-interest is user 1, the expression of ϵ is given by

$$\epsilon = \frac{C_1(k_1) - \sum_{q=2}^{Q} C_q(k_1)}{N_f^2} \tag{25}$$

Table 1 shows several examples of the set of TH codes for 4-emitter case that result in different efficiency factors. The TH assignment considers $N_h = 11$ and the user-of-interest is user 1.

Table 1. TH codes assignment for 4-emitter case.

User 1	User 2	User 3	User 4	ϵ
{3,2,3,6}	{4,8,1,7}	{2,0,4,0}	{10,10,8,10}	1
{0,8,9,4}	{9,1,4,2}	{7,3,1,3}	{8,9,0,10}	0.8
{9,0,7,1}	{1,6,8,4}	{7,7,5,7}	{3,4,9,0}	0.5
{6,7,6,8}	{2,4,3,5}	{3,9,7,1}	{7,1,4,10}	0.3
{3,6,3,2}	{9,4,9,4}	{4,7,7,10}	{7,1,1,9}	0.1

4.2. Multipath Channel

In a multipath channel, the received signal at one sensor is no longer a delay-shifted received signal at the other's sensor; instead, it differs from one sensor to the other because of the DoA of each multipath component. Therefore, the technique used in previous section is theoretically invalid. To overcome this, we utilize a simple level-thresholding detector (LTD) structure to detect the first-arrival multipath component.

The LTD structure is implemented after RF front-end of each sensor and its block diagram is shown in Figure 4. It consists of an analog comparator and a latch circuitry. The analog comparator senses the incident when the received signal crosses the level threshold γ. When it is sensed, the latch circuitry will be triggered and generate a rectangular pulse through latching process. During the latching, the incidents when the received signal crossing the threshold do not trigger the generation of the rectangular pulse. Hence, the first-arrival multipath component is expected to cross the threshold before the subsequent-arrival multipath component. This is true only when the following condition is satisfied

$$\tau_l^{(q)} + \tau_{l,n}^{(q)} < T_{latch} \qquad \text{for } \{1 \le l \le L_q \big| a_l^{(q)} > \gamma, \forall q\} \tag{26}$$

where T_{latch} is the latching duration. That means, only the incident when the first-arrival multipath component arrives triggers the generation of the pulse. This way, the DOA of the first-arrival

multipath component is captured at the rising time of the rectangular pulse.

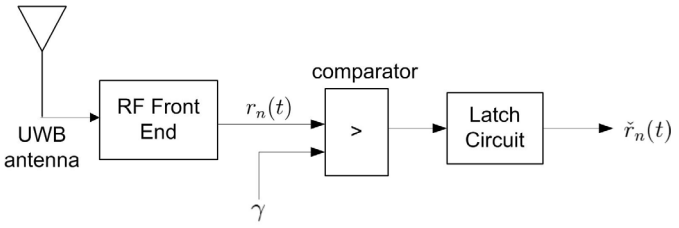

Figure 4. The block diagram of the LTD used at the RF front-end of each sensor. It consists of an analog comparator and a latch circuitry.

Let $\check{r}_o^{(q)}(t)$ denote the output of the LTD at the n-th sensor, the sum of these LTDs' output can be expressed as

$$\check{r}_o^{(q)}(t) = p(t - \tau_{toa}^{(q)} - \tau_l^{(q)} \tag{27}$$

where $p(t)$ is the rectangular pulse waveform.

With the implemented LTDs, the sum of the received signal at the array $y(t)$ now contains only one DoA for every transmitted pulse and the technique described in Section 4.1 can be used to cancel the MAI. However, because the LTD is subjected to error when noise is present and/or (27) is not satisfied, the DoA estimated may also be erroneous. When we present the simulation results, we will investigate the effectiveness of the proposed method in the presence of such errors.

5. NUMERICAL RESULTS

In this section, simulation results are presented to assess the performance of the proposed method for both the AWGN and multipath cases. Table 2 describes the parameters used in all simulations presented. We consider an N-element uniform linear array (ULA) with inter-element spacing d, where the first element is located at the array phase center.

Considering that extremely high sampling rate (50 GHz) is used to simulate the received signal in analog domain, the sum of the received signals at the array is channelized into M-frequency channelizer using the structure shown in Figure 2 with the parameters listed in Table 3. Each branch of the channelizer consists of a complex mixer, Bessel band pass filter and analog-to-digital converter of f_s sampling frequency.

Table 2. Simulation parameters.

Parameter	Value
Baseband pulse waveform	Gaussian 2^{nd} derivative
Pulse duration / width	1 ns / 0.4 ns
TH-SS multiple access	$T_f = 80$ns, $T_c = 10$ns and $N_f = 4$
Receiving array	ULA with $N = 7$ and $d = 50\,\text{cm}$
Numer of emitters	2
TH sequence	$c_j^{(1)}$ and $c_j^{(2)}$
Signal DoA with respect to the array axis	30° and 56°

Table 3. Channelization parameters.

Parameter	Value
Number of branches M	5
Bessel band pass filter	5^{th} order with $f_o = 12.5$MHz and 1 kHz bandwidth
ADC sampling rate f_s	$4f_o$
Number of snapshots	$T_f \times N_f \times 4f_o$ (one symbol period observation)

5.1. AWGN Channel

We first demonstrate the effectiveness of the proposed method in an AWGN propagation channel by considering two emitters transmission, each employs TH-SS multiple access technique of different TH code ($c_j^{(1)} = \{5, 5, 2, 2\}$ and $c_j^{(2)} = \{0, 6, 4, 2\}$). The emitters are located at different directions, measured with respect to the array axis. The path loss attenuation experienced by both emitters is assumed to be equal. The simulation considered signal-to-noise ratio (SNR) of 0 dB.

Figure 5 shows the plot of the normalized DF function, defined as $\text{DF}(\theta_s) = |\mathbf{P}_{\bar{C}}^{\perp}(\theta_s)\mathbf{y}|^{-1}$. It can be observed that different plots are shown for different frequencies selected for the channelizer. If user 1 (2) is the user-of-interest, the frequencies are selected from the subset of $f^{(1)}$ ($f^{(2)}$). Each plot successfully indicates the DoA of the respective emitter.

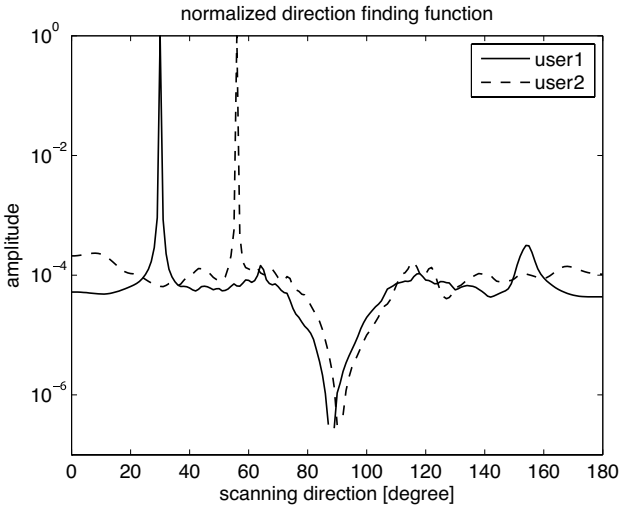

Figure 5. Normalized DF function plotted as a function of the scanning direction. The results are obtained using the parameters in Table 1 and 2. The solid and dotted lines is obtained from setting the channelizer's frequencies to be the subset of $f^{(1)}$ and $f^{(2)}$, respectively.

5.2. Multipath Channel

The multipath (temporal) channel model considered is generated with the parameters suggested in [11]. To generate the received multipath signals at the array, the simulation requires the spatial information as well. To incorporate the spatial information into the channel impulse response (CIR), we utilized the model proposed by [12], which is subsequently conceded by [13]. It is derived from the assumption that the temporal and spatial information is statistically independent. Because the temporal CIR is modeled using a cluster-ray model, the spatial information should follow this model. The DoAs of the clusters are generated as random variables following uniform distribution while those of the rays are generated as random variables following Laplacian distribution. The uniformly distributed random variables range from 0° to 180° due to the ULA geometry. For every cluster generated, several rays need to be generated. Their distribution is centered at the cluster's DoA with 25.5° standard deviation. Figure 6 shows an example of the simulated spatio-temporal CIR.

Using the spatio-temporal CIR, we can generate the received multipath signals at the array. Because each emitter experiences different propagation, the simulation needs to generate multiple CIR

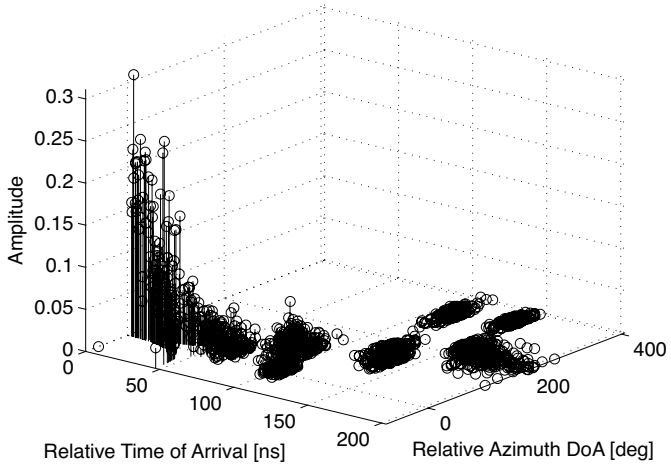

Figure 6. A simulated spatio-temporal CIR of indoor office/laboratory environment. The model considers CM3 model [11] and incorporates the spatial information.

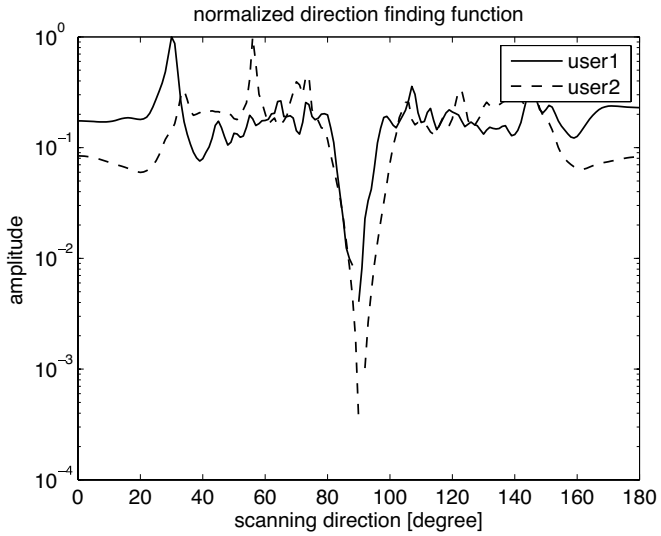

Figure 7. Normalized direction finding function plotted as a function of the scanning direction for the multipath case. Although the errors in the estimated differential delays cause the multiple small peaks, the main peak correctly indicates the desired DoA.

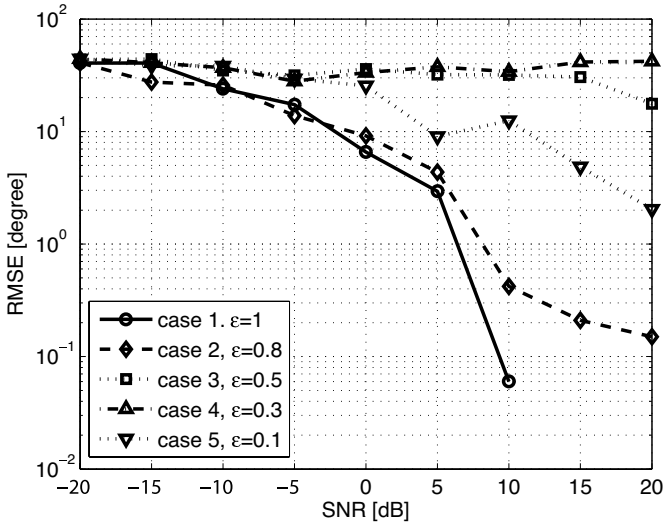

Figure 8. Plots of RMSE versus SNR for different sets of TH codes as listed in Table 1. These sets give different efficiency level. Both case 1 and 2 show a relatively good estimation.

to simulate the received multipath signals at the array due to multiple emitters' transmission.

The thresholds for the LTDs simulated are equally set at 0.3 and the latching duration T_{latch} is half of the chip duration. Figure 7 shows the normalized DF function for the case of multipath channel. Because of the presence of errors in the estimated value of the differential delay $\tau_{1,n}^{(q)}$, multiple small peaks are observed surrounding the main peak. The differences between these peaks and the main peak are much smaller as compared to the normalized DF function for the AWGN case. Nevertheless, the proposed method successfully estimates the desired DoA

5.3. RMSE Performance

In this section, we evaluate the performance of the proposed method for the multipath case in terms of root mean square error (RMSE). The RMSE value is calculated from the estimation errors of 100 different realizations, but the generated CIR is the same for every realization.

First, we consider simulating the proposed method for the AWGN case with 3 emitters as the MAI. The simulation uses the set of TH codes listed in Table 1 to investigate the effect of the reduced ϵ on

the proposed method. Figure 8 shows the RMSE performance as a function of SNR for different value of ϵ. The first set of the TH codes listed in Table 1 that gives $\epsilon = 1$ is considered as Case 1. Case 2, 3, 4 and 5 are the sets that gives $\epsilon = 0.8, 0.5, 0.3$ and 0.1, respectively. It is shown that the estimator is able to provide a reliable estimation for both Case 1 and 2. It implies that a maximum efficiency is preferred when designing the set of TH codes, but not a must. A 0.2 tolerance value is acceptable. Hence, the design of the TH codes is relaxed.

6. CONCLUSION

In this paper, an extension of channelizer-based UWB DoA estimation to the case for multiple emitters has been proposed. Assuming that the emission of the UWB signal follows the ideal TH-SS multiple access scheme, the DoA estimation can be tailored to single emitter estimation with prior knowledge of the respective TH code and the TH codes of the other emitters. The simulation presented has considered the presence of two emitters of different TH codes transmitting UWB signal concurrently. The results show a perfect estimation under multipath-free condition. In a multipath environment, we have proposed the use of analog LTDs to detect the first-arriving multipath component. By summing the LTDs' output, the estimation has been shown to be accurate despite the presence of the errors in detection.

ACKNOWLEDGMENT

The material in this paper was presented in part at IEEE WiCOM 2005.

APPENDIX A. DERIVATION OF $C_Q(F)$

The definition of $C_q(f)$, given in (21), can be expressed as

$$C_q(f) = \left| \sum_{j=0}^{N_f-1} \exp[-i \underbrace{2\pi f(jT_f + c_j^{(q)} T_c)}_{\varphi_j}] \right|^2 \tag{A1}$$

The exponent term inside the sum can be expanded using Euler's formula and further simplified as follows

$$C_q(f) = \left| \sum_j \{\cos(\varphi_j) + i\sin(\varphi_j)\} \right|^2 \tag{A2}$$

$$C_q(f) = \left\{ \sum_j \cos(\varphi_j) \right\}^2 + \left\{ \sum_j \sin(\varphi_j) \right\}^2 \tag{A3}$$

$$\begin{aligned} C_q(f) = & \sum_j \left\{ \cos^2(\varphi_j) + \sin^2(\varphi_j) \right\} \\ & + \sum_{j_1} \sum_{j_2} \{\cos(\varphi_{j_1})\cos(\varphi_{j_2}) + \sin(\varphi_{j_1})\sin(\varphi_{j_2})\} \\ & j_1 \neq j_2 \end{aligned} \tag{A4}$$

Utilizing the following two trigonometry identities

$$\begin{aligned} \cos^2(A) + \sin^2(A) &= 1 \\ \cos(A_1)\cos(A_2) + \sin(A_1)\sin(A_2) &= \cos(A_1 - A_2) \end{aligned} \tag{A5}$$

we can now expressed $C_q(f)$ as

$$C_q(f) = N_f + \sum_{j_1} \sum_{j_2} \cos(\varphi_{j_1} - \varphi_{j_2}) \tag{A6}$$

Using the definition of ρ_q in (22), we have

$$\varphi_{j_1} - \varphi_{j_2} = 2\pi f \rho_q T_c \tag{A7}$$

With the above two equations, we will arrive at the simplified expression of $C_q(f)$ in (23).

REFERENCES

1. Lie, J. P., C. M. See, and B. P. Ng, "Ultra wideband direction finding using digital channelization receiver architecture," *IEEE Communications Letters*, Vol. 10, No. 2, 79–81, Feb. 2006.
2. Win, M. Z., "A unified spectral analysis of generalized time-hopping spread-spectrum signals in the presence of timing jitter," *IEEE J. Selected Areas in Communications*, Vol. 20, No. 9, 1664–1676, Dec. 2002.

3. Win, M. Z. and R. A. Scholtz, "Ultra-wide bandwidth time-hopping spread-spectrum for wireless multiple access communications," *IEEE Transactions on Communications*, Vol. 48, No. 4, 679–689, Apr. 2000.
4. Win, M. Z., R. A. Scholtz, and M. A. Barnes, "Ultra-wide bandwidth signal propagation for indoor wireless communications," *IEEE Proc. Int. Conf. Communications*, Vol. 1, No. 4, 55–60, 1997.
5. Xiao, S. Q., J. Chen, B. Z, Wang, and X. F. Liu, "A numerical study on time-reversal electromagnetic wave for indoor ultra-wideband signal transmission," *Progress In Electromagnetics Research*, PIER 77, 329–342, 2007.
6. Fontana, R. J. and S. J. Gunderson, "Ultra wideband precision asset location system," *Proc. IEEE Int. Conf. on Ultra Wideband Systems and Technologies*, 2002.
7. Soliman, M. S., T. Morimoto, and Z.-I. Kawasaki, "Three-dimensional localization system for impulsive noise sources using ultra-wideband digital interferometer technique," *Journal of Electromagnetic Waves and Applications*, Vol. 20, No. 4, 515–530, 2006.
8. Chen, C.-H., C.-L. Liu, C.-C. Chiu, and T.-M. Hu, "Ultra-wide band channel calculation by SBR/image techniques for indoor communication," *Journal of Electromagnetic Waves and Applications*, Vol. 20, No. 1, 41–51, 2006.
9. Landesa, L., I. T. Castro, and J. M. Taboada, "Bias of the maximum likelihood DOA estimation from inaccurate knowledge of the antenna array response," *Journal of Electromagnetic Waves and Applications*, Vol. 21, No. 9, 1205–1217, 2007.
10. Vescovo, R., "Beam scanning with null and excitation constraints for linear arrays of antennas," *Journal of Electromagnetic Waves and Applications*, Vol. 21, No. 2, 267–277, 2007.
11. Foerster, J., "Channel modeling sub-committee report final," IEEE802.15-02/490.
12. Spencer, Q., M. Rice, B. Jeffs, and M. Jensen, "A statistical model for the angle-of-arrival in indoor multipath propagation," *Proc. IEEE Vehicular Technology Conference*, Vol. 3, 1415–1419, 1997.
13. Cramer, R. J-M., R. A. Scholtz, and M. Z. Win, "Evaluation of an ultra-wide-band propagation channel," *IEEE Transactions on Antennas and Propagation*, Vol. 50, No. 5, 561–570, May 2002.